Int. J. Electrochem. Sci., 10 **(2015)** 5276 - 5290

International Journal of
ELECTROCHEMICAL
SCIENCE
www.electrochemsci.org

Effect of UV-A Irradiation and Temperature on the Antioxidant Activity of Quercetin Studied Using ABTS, DPPH and Electrochemistry Methods

Anna Masek[1,*], *Ewa Chrzescijanska*[2]

[1]Technical University of Lodz, Institute of Polymer and Dye Technology, Faculty of Chemistry, 90-924 Lodz, ul Stefanowskiego 12/16, Poland
[2]Technical University of Lodz, Institute of General and Ecological Chemistry, Faculty of Chemistry, 90-924 Lodz, ul Zeromskiego 116, Poland
[*]E-mail: anna.masek@p.lodz.pl

Received: 13 April 2015 / *Accepted:* 14 May 2015 / *Published:* 27 May 2015

The electrochemical oxidation of quercetin was investigated at a Pt electrode using the voltammetry methods. Quercetin is irreversibly oxidized in at least three electrode steps. The effects of the scan rate (v) and substrate concentration (c) on the electrooxidation were determined. Cyclic voltammograms of quercetin oxidation were recorded and the following parameters were determined: peak potential (E_p), half-peak potential ($E_{p/2}$), half-wave potential ($E_{1/2}$), anodic peak currents (i_{pa}). The following parameters were calculated: transfer coefficients ($\beta_{n\beta}$) and electrode reaction rate constants (k_{bh}). The investigation results prove the exchange of one electron and one proton in the first step followed by a chemical reaction. The hydroxyl group of ring B at position 3′ is oxidized. Quercetin electrooxidation occurs according to the EC mechanism. Then, the hydroxyl group of ring B at position 4′ is oxidised. The i_{pa} is linear with the quercetin concentration. Considering the investigation results and quantum chemistry calculations, the quercetin electrooxidation mechanism was proposed. Electrochemistry and radical scavenging methods confirmed the high antioxidant activity of quercetin. The stability of quercetin against photooxidation (irradiation UVA) and thermooxidation is relatively high. FTIR spectrum shows no significant changes after ageing in the structure of quercetin. Quercetin exhibited good reduction properties in the oxidation process.

Keywords: Quercetin; Electrochemical oxidation; Cyclic voltammetry; Differential pulse voltammetry

1. INTRODUCTION

Quercetin is a flavonoid a group of polyphenolic compounds and present in plants and food of plant origin [1]. It has anti-cancer [2], anti-inflammatory [3, 4] and anti-allergic properties. Most of

these beneficial effects are known because of the antioxidant activity [6, 7]. The structure of quercetin is shown in Figure 1.

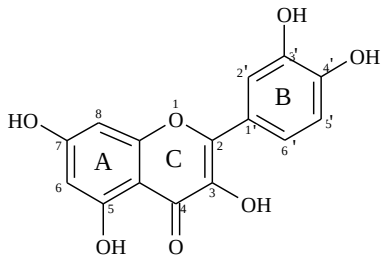

Figure 1. Molecular structure of quercetin.

Quercetin has the general structure of a 15-carbon skeleton, which consists of 2 phenyl rings and a heterocyclic ring. Therefore, the study of the properties of quercetin and the development of a selective, simple and accurate method for the detection are very important.

The main methods to determine quercetin are chromatographic methods such as gas chromatography coupled with mass spectrometry, liquid chromatography mass spectrometry, and capillary electrophoresis with electrochemical detection. Although chromatographic methods provide low detection limits, they require a lot of time and complicated and expensive analytical equipment. It is very important to develop a convenient and fast analytical method to determine quercetin. The application of conventional electrochemical methods with a simple change of the electrode surface can achieve those objectives. In this work, we attempt to show that using the conventional electrochemical methods with a platinum electrode can achieve these goals.

Furthermore, electron transfer processes with antioxidant participation that occur on the electrode surface and in living cells are related in some aspects. Therefore, electrochemical methods are widely used to investigate and determine antioxidants [8-10]. The commonly used electrochemical methods are cyclic voltammetry (CV), linear sweep voltammetry (LSV), differential pulse voltammetry (DPV)) and square-wave voltammetry (SWV) [11-14]. They have advantages over other analytical methods, such as [15-23] no requirement for excessive sample preparation, instrumentation simplicity and portability (facile miniaturization), high accuracy, sensitivity, selectivity and reproducibility, fast response, cost effectiveness (low power requirements), and possibility of detecting multiple analytes without separation steps. Among the electroanalytical methods, voltammetry appears particularly suitable to determine and characterise the electrochemical behaviours of various compounds [23]. Voltammetric methods allow for the determination of parameters such as anodic and cathodic peak currents, total charge below the peaks, and oxidation and reduction potentials (half-wave potential), among others. These parameters can be used in qualitative analyses of compounds and assessment of their antioxidant and redox properties. Additionally, voltammetric methods are important in the determination of the electrode reaction mechanism of flavonoids [24-26]. In the electrochemical determination and characterization of various compounds, particularly organic compounds, the selection of a working electrode material is critical to the experimental results. Various electrode materials, e.g., mercury, solids and modified electrodes, are applied in

electroanalytical measurements. However, platinum appears to be one of the most suitable electrode materials because of its good electrochemical inertness and ease of fabrication into many forms.

The investigation aimed to determine the electrochemical behaviour of quercetin at a platinum electrode. The application of the Pt electrode is the initial stage in our investigations for comparison with other electrode materials, which will be used in quercetin electrooxidation. The effects of the scan rate and substrate concentration on the quercetin electrode reactions were investigated. CV and DPV techniques were applied in the investigations.

2. EXPERIMENTAL

2.1. Chemicals

The subject of the investigation was quercetin (3,3′,4′,5,7-pentahydroxyflavone, $C_{15}H_{10}O_7$) purchased in Sigma-Aldrich (Germany). The chemical that was used to prepare the quercetin solutions was acetonitrile (CH_3CN) pure p.a. (Sigma-Aldrich, Germany). Its non-aqueous solutions were prepared by dissolving the substrate in the supporting electrolyte (0.1 mol L^{-1} $(C_4H_9)_4NClO_4$, Fluka, France). The concentration of quercetin solutions varied from 0.5×10^{-3} to 2×10^{-3} mol L^{-1}. All the reagents used were of analytical grade.

2.2. Measurement methods

2.2.1. Ageing treatment of quercetin

Quercetin was subjected to the action of air at an elevated temperature (383 K) for 10 days in a dryer with thermo-circulation. UV aging was performed using a UV 2000 apparatus from Atlas. The tests lasted for 288 h and consisted of two alternately repeating segments: a day segment (radiation intensity 0.7 W/m2 (λ= 340 nm; temperature 60°C; duration 8 h) and a night segment (no UV radiation; temperature 50°C; duration 4 h).

2.2.2. Cyclic and differential voltammetry

Electroanalytical measurements were carried out using an Autolab PGSTA30 Electrochemical Analyzer (EcoChemie, The Netherlands). A three-electrode electrochemical cell employed in measurements consisted of a reference electrode, an auxiliary electrode (platinum wire) and a working electrode - platinum with geometric surface area of 0.5 cm^2. A potential of the working electrode was measured vs. ferricinium/ferrocene electrode (Fc^+/Fc). Before measurements in quercetin solution, Pt electrode was rinsed thoroughly in acetonitrile. Determination of qercetin and kinetic parameters of its electrode reactions was performed using CV and DPV voltammetry. CVs were recorded in the potential from 0 to 1.5 or 2.0 V with various scan rates (0.01 to 2.0 V s^{-1}). DPVs were recorded in the same potential range with modulation amplitude 25 mV, pulse width 50 ms (scan rate 0.01 V s^{-1}). Prior to the measurements, the solutions were purged with argon in order to remove dissolved oxygen.

During measurements argon blanket was kept over solutions. All experiments were carried out at room temperature.

The quantum chemical calculations were performed using the AM1 method with HyperChem program packages.

2.2.3. Scavenging of DPPH radicals

The antioxidant activity of quercetin was evaluated toward the DPPH radical. The ethanol solution of the DPPH (2.0 ml) with a concentration of 40 mg/ml (0.1 mM) was added to 0.5 ml of an ethanol solution (70% ethanol) that contained 0.02 mg/ml quercetin. Then, minutes after mixing, the absorbance of the solutions was spectrophotometrically determined at 516 nm using a UV-visible Spectrometer. As a blank, 70% ethanol was used. The inhibition level (%) of DPPH was calculated using the following equation:

$$\text{Inhibition (\%)} = [(A_o - A_1)/A_o] \times 100 \quad (1)$$

where A_o was the absorbance of the control and A_1 was the absorbance in the presence of the sample of quercetin [27, 28].

2.2.4. Scavenging of ABTS radicals

The antioxidant activity of quercetin was investigated using the $ABTS^{\bullet+}$ method. ABTS was dissolved in water to a 6 mM concentration and then mixed with 2.45 mM potassium persulfate. The mixture was left in the dark at room temperature for 15 h before use. The ABTS /radical solution was diluted with ethanol to an absorbance of 0.70 at 734 nm. After the diluted $ABTS^{\bullet+}$ solution (6.0 ml) was mixed with a 50 μL aliquot of each investigated solution (6 mg/ml) or Trolox in ethanol, the absorbance was measured at 734 nm after 2 min at 24 ºC. The inhibition level (%) of absorbance was obtained using the standard curve, which was prepared with Trolox (% inhibition level- μM Trolox). The capability of quercetin on scavenging $ABTS^{\bullet+}$ was the Trolox equivalent antioxidant capacity (TEAC) [29,30]

2.2.5. FTIR analysis

FTIR spectra were tested in the range of 3000 – 700 cm^{-1} using an FTIR Nicolet 6700 FTIR (Thermo Scientific). The measurement parameters were as follows: 280 scans; resolution was set to 8 cm^{-1}; DTGS/KBr detector was employed. The FTIR spectrum of the compound was also recorded in the range of 3500 – 1000 cm^{-1}.

2.2.6. Thermogravimetry

The thermogravimetric analysis (TGA) was using Mettler Toledo (Mettler-Toledo, Schwarzenbach, Switzerland). Samples with a total weight in the 7-10 mg range were placed into

alumina crucibles and subjected to a temperature program used from 20 to 500 ºC at a heating rate of 10 ºC min^{-1} in an nitrogen atmosphere (flow rate of 50 mL min^{-1}).

3. RESULTS AND DISCUSSION

3.1. Cyclic and differential pulse voltammetric behaviours of quercetin

The electrooxidation of quercetin was investigated at the platinum electrode using CV and DPV methods. CV is one of the universally used methods to study and analyse compounds. It is not sufficiently sensitive for trace amount determination of antioxidants but is useful to optimize the analytical conditions, provides some important information about the oxidation mechanism of the active principles and allows for the determination of antioxidants as the major components [31, 32].

To check whether the substrate is adsorbed at the electrode, differential pulse voltammograms (DPVs) were recorded. DPV is usually based on the staircase excitation waveform. The fixed-magnitude pulses, which are superimposed on a linear potential ramp, are applied to the working electrode. The current is measured twice in each pulse period (before and at the end of the pulse). The difference between these two currents is recorded and displayed as a function of the potential, which allows one to diminish surface effects such as adsorption on the electrode. DPV is one of the most sensitive voltammetric techniques. The analytical signal has the form of a peak, which is suitable for analytical purposes [33-35].

Example voltammograms are shown in Figure 2. The electrooxidation of quercetin was investigated in the potential range, where a supporting electrolyte showed no peaks (Fig. 2, curve 3).

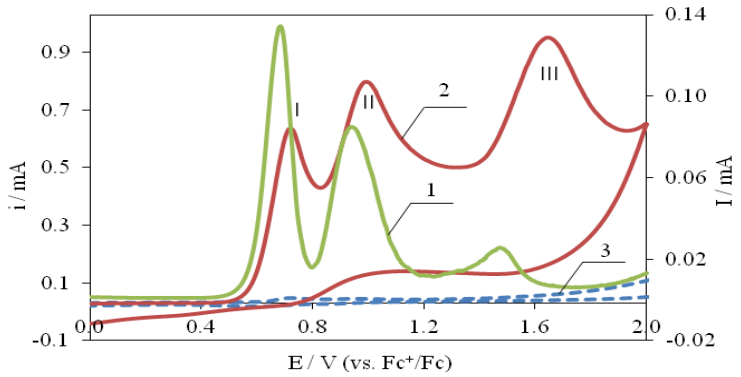

Figure 2. Voltammograms for 2×10^{-3} mol L^{-1} quercetin in 0.1 mol L^{-1} $(C_4H_9)_4NClO_4$ in acetonitrile, v = 0.1 V s^{-1}; curve 1 - DPV, 2 - CV, 3 - CV recorded in the supporting electrolyte.

The voltammograms in Fig. 2 (curves 1 and 2) show that quercetin is probably irreversibly oxidised in at least three electrode steps at potentials lower than the electrolyte decomposition potentials. The value of E_p that was determined from the DPV should correspond to $E_{1/2}$ from CV. The three peaks that appear in the DP voltammogram (Fig. 2, curve 1) prove the lack of adsorption and diffusive character of quercetin electrooxidation. The half-wave potential ($E_{1/2}$) of quercetin

electrooxidation, which was determined from the cyclic voltammogram (CV), is 0.68 V for peak I, 0.95 V for peak II, and1.47 V for peak III. These values correspond to the peak potential (E_{pa}) that was determined from the differential pulse voltammogram (DPV). The value of $E_{1/2}$ shifted with an increase in the scan rate towards more positive values, which shows the increasing irreversibility of the process.

3.2. An effect of the scan rate

The relationship between the peak current and the scan rate delivers information about the electrochemical mechanism of electrooxidation or electroreduction. Therefore, the effect of the scan rate on the potentials and currents of both peaks I and II was examined in the range of 0.01-2 V s^{-1}.

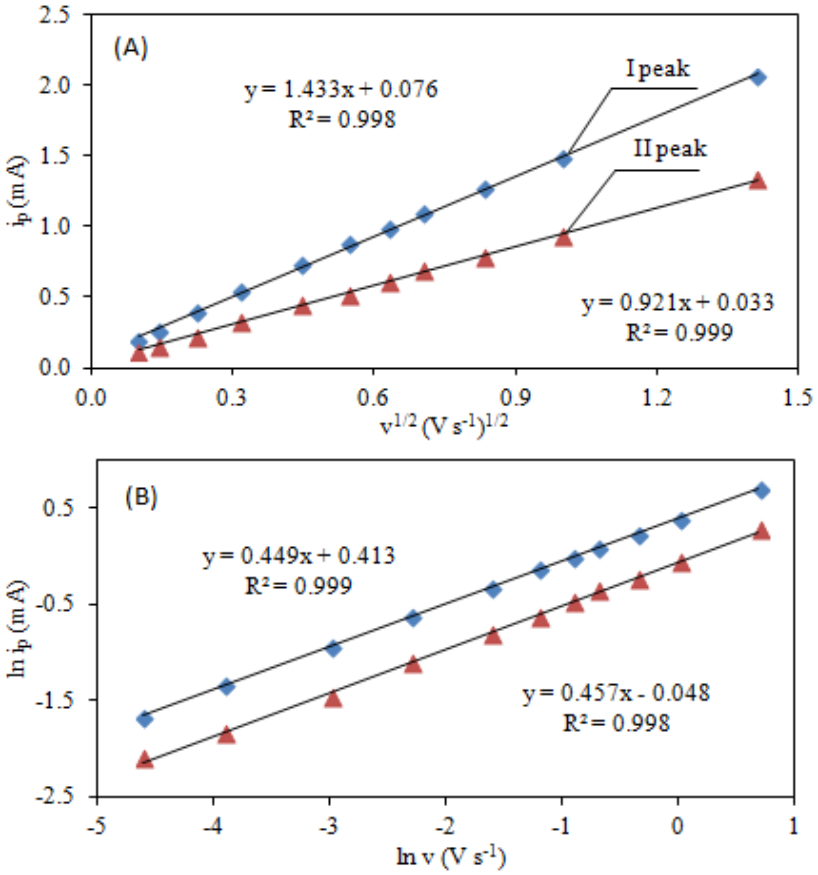

Figure 3. (**A**) Dependence of $i_p = f(v^{1/2})$. (**B**) Dependence of ln i_p = f (ln v) for the oxidation of quercetin at a Pt electrode in 0.1 mol L^{-1} $(C_4H_9)_4NClO_4$ in acetonitrile; c = 2×10^{-3} mol L^{-1}.

Two approaches that are widely used to study the reversibility of reactions and to determine whether a reaction is adsorption-controlled or diffusion-controlled are the analysis of the dependence of i_p on $v^{1/2}$ and the analysis of the dependence of ln i_p on ln v. Cyclic voltammograms were used to determine the peak current and potential for the quercetin electrooxidation. Figure 3 shows this relationship for the first and second steps of quercetin electrooxidation in $(C_4H_9)_4NClO_4$ in acetonitrile.

The peak currents of peaks I and II linearly increased with $v^{1/2}$ following the relationships:

i_{p1} (mA) = 1.433 $v^{1/2}$ $(Vs^{-1})^{1/2}$ + 0.076 $R^2 = 0.998$ for peak I

i_{p2} (mA) = 0.921 $v^{1/2}$ $(Vs^{-1})^{1/2}$ + 0.033 $R^2 = 0.999$ for peak II

which suggests that the electrooxidation of quercetin can be controlled by diffusion or adsorption.

In addition, the plot ln i_p *vs* ln *v* exhibits the slopes of 0.449 and 0.457 for peaks I (ln i_{p1} = 0.449 ln *v* + 0.413; R^2 = 0.999) and II (ln i_{p2} = –5.04 + 0.457 ln *v* – 0.048; R^2 = 0.998), respectively. This result confirms that the mass transfer process is diffusion-limited because the slope must be equal to 0.50 for diffusion control and approaches 1.0 for adsorption-controlled processes [36].

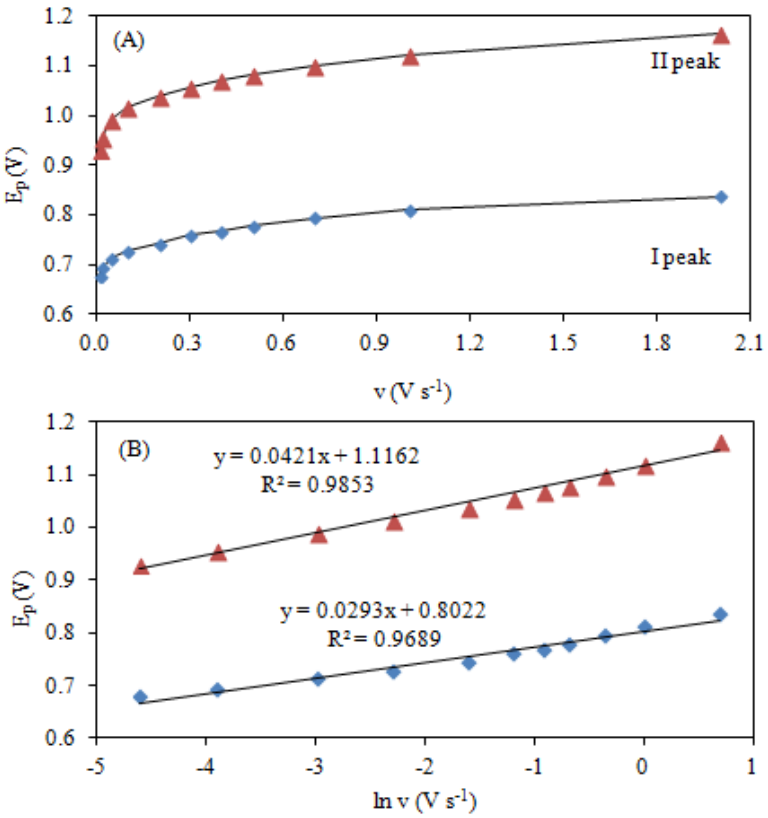

Figure 4. (A) Dependence of anodic peak potential (E_p) on the scan rate (*v*) for the oxidation of quercetin at a Pt electrode. (B) Relationship between anodic peak potential (E_p) and logarithm of scan rate (ln *v*); c = 2 × 10^{-3} mol L^{-1} in 0.1 mol L^{-1} $(C_4H_9)_4NClO_4$ in acetonitrile.

An effect of the scan rate on the quercetin electrooxidation potential was also investigated. Figure 4(A) shows the dependencies of the peak potential (E_p) vs. the scan rate (v) for quercetin electrooxidation. For both peaks, the increase in scan rate promoted slight displacements in the peak potential towards more positive values, which proves the irreversible character of both processes. Thus, it can be concluded that both irreversible and diffusion-controlled mass transport processes occur. Further analysis of the quercetin electrooxidation (the anodic peaks) included determining the $i_{pa}/v^{1/2}$ vs. v dependence for quercetin electrooxidation. This dependence is shown in Figure 5.

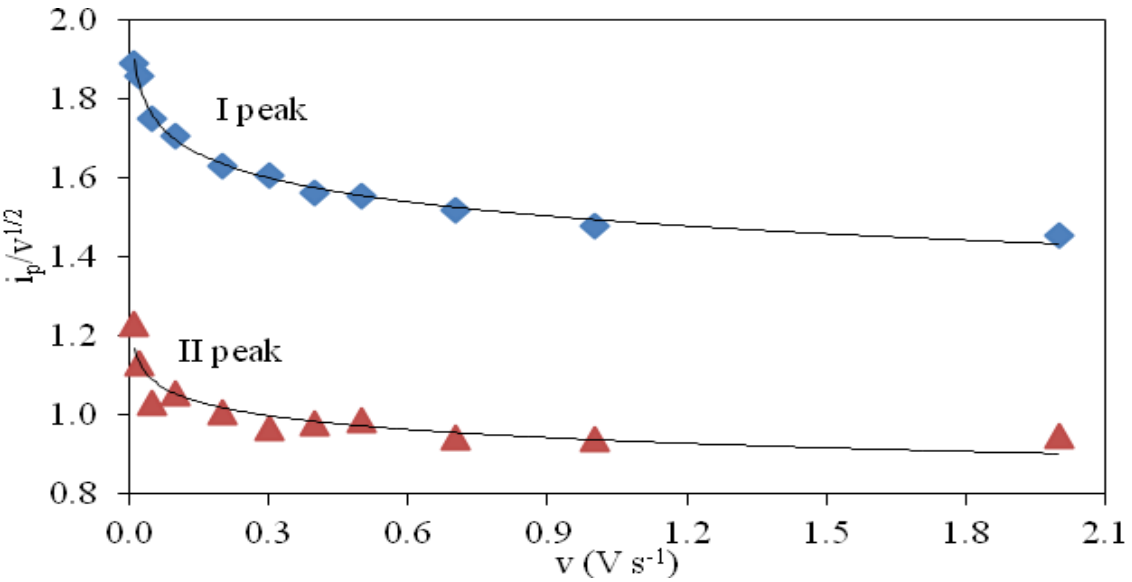

Figure 5. Variation of the scan rate normalized current ($i_{pa}/v^{1/2}$) with scan rate for the oxidation of qercetin at a Pt electrode; c = 2 × 10^{-3} mol L^{-1} in 0.1 mol L^{-1} $(C_4H_9)_4NClO_4$ in acetonitrile.

The scan-rate-normalised current ($i_p/v^{1/2}$) function clearly depends on v. If the process is reversible or irreversible without a preceding or following chemical reaction, the dependence on v should not be observed [37]. The shape of this dependence (Fig. 5) for the anodic peaks of the quercetin electrooxidation is typical for an EC mechanism [38-41].

Moreover, the electron transfer coefficient for the quercetin electrooxidation reaction was calculated according to the following equation (1) [40, 42-43]:

$$E_p = \left(\frac{RT}{2\beta n_\beta F}\right)\ln v + const \qquad (1)$$

where E_p is the peak potential (V), R is the universal gas constant (8.314J K^{-1} mol^{-1}), F is the Faraday constant (96,487 C mol^{-1}), T is the Kelvin temperature (298 K), βn_β is the anodic transfer coefficient, and v is the scan rate (V s^{-1}).

This equation can be applied in the case of a totally irreversible diffusion-controlled process. A dependence of E_p vs. ln v is presented in Fig. 4B. The total value of βn_β is 0.44 for peak I and 0.31 for peak II.

3.3. The effect of the quercetin concentration on the substrate electrooxidation

The effect of the quercetin concentration on its electrooxidation was investigated in the range of 0.5 × 10^{-3} to 2.0 × 10^{-3} mol L^{-1}. The CV curves were recorded with a scan rate of 0.1 V s^{-1}. The dependence of the oxidation peak current on the concentration is shown in Figure 6.

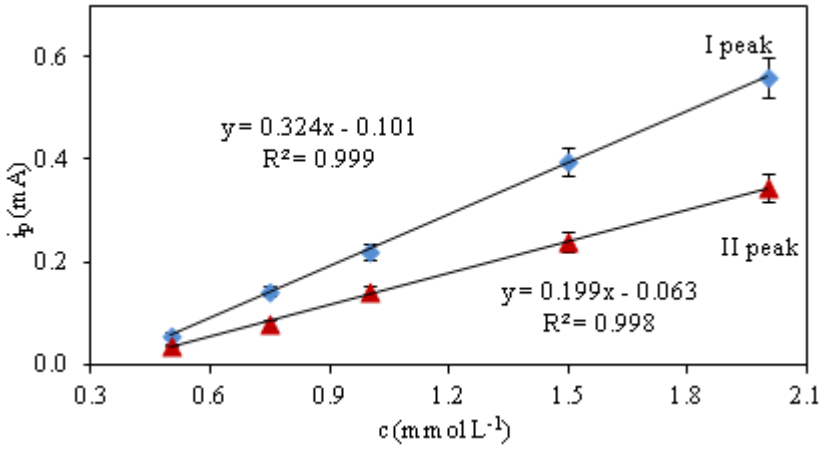

Figure 6. Plot of the anodic peak current (i_p) versus concentration of quercetin; v = 0.1 V s^{-1}.

The dependence $i_p = f(c)$ is linear for the tested concentrations and described using the following equations:

$i_p = 0.324[c\ (mmol\ dm^{-3})]$ mA - 0.101 mA $R^2 = 0.999$ for I peak

$i_p = 0.199[c\ (mmol\ dm^{-3})]$ mA - 0.063 mA, $R^2 = 0.998$ for II peak.

Because of the linearity of i_p vs. quercetin concentration, the cyclic voltammetry method can be successfully applied to determine the quercetin concentration [44, 45]. The recorded cyclic voltammograms for different substrate concentrations were used to determine the peak potential (E_{pa}), half-peak potential ($E_{pa/2}$) and half-wave potential ($E_{1/2}$) for peaks I and II of the quercetin electrooxidation. Based on the determined values, the anodic transfer coefficient (βn_β) and heterogeneous rate constant (k_{bh}) were calculated according to equations in [46, 47]. The half-wave potential of step I ($E_{1/2}$) is 0.72 V and that of electrode II is 0.98 V. The βn_β for peaks I and II of the quercetin electrooxidation is 0.51±0.05. The k_{bh}, which was determined at the half-wave potential, is $(4.5\pm0.2) \times 10^{-4}$ cm s^{-1}.

3.4. Quercetin oxidation processes

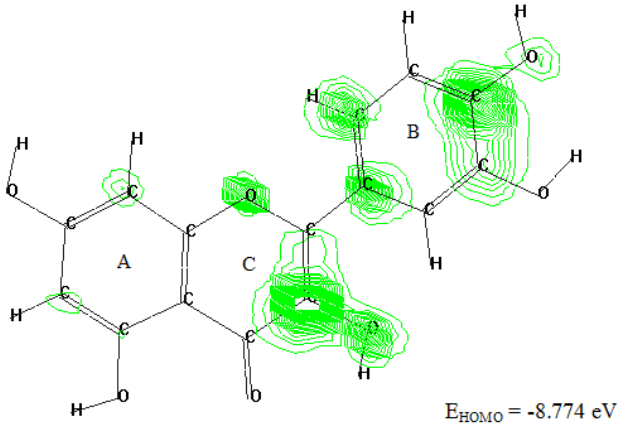

Figure 7. Molecular orbital representation of quercetin.

The obtained electrooxidation kinetic parameters can be compared using quantum-chemical calculations [48, 49]. The molecular orbital energy (E_{HOMO}) was calculated using the AM1 method as determined in the HyperChem software. The calculated energy of the highest filled orbital (E_{HOMO} − ionisation potential) determines tendency of molecule to donate electrons. The distribution of electron charges in a molecule indicates the sites that are most susceptible to oxidation (Fig. 7).

The structure of quercetin has -OH groups attached to the rings, which can be electrochemically oxidized. From Figure 7, we find that the distribution of electron of quercetin is mainly distributed in the B-ring and less in the C-ring, which suggests the ease of oxidation of the hydroxyl groups in these rings. Thus, the higher ability to respond to the functional site is mainly focused on the B-ring and the conjugate part. The electron-donating capability of a molecule can be determined by the HOMO values; a high HOMO corresponds to a strong capability to donate electrons. E_{HOMO} for quercetin is -8.646 eV.

The oxidation of quercetin in subsequent electrode steps are connected with the number of hydroxyl groups and their positions in the three aromatic rings of this compound. Quercetin has two hydroxyl groups in ring B, two hydroxyl groups in rings A and one hydroxyl group in ring C [50]. The quercetin oxidation processes proceed in three steps. First, the hydroxyl groups are oxidized in ring B, which corresponds to peaks I and II (Fig. 2). With the least potential (the first step), the hydroxyl group of ring B at position 3′ is oxidised, and one electron and one proton are exchanged (peak I). Then, the hydroxyl group of ring B at position 4′ is oxidised (peak II). The hydroxyl group at position 3 in ring C is subsequently oxidised, which corresponds to peak III (Fig. 2). The hydroxyl groups at positions 5 and 7 in ring A also have an electron-donating effect, but oxidation is more difficult here (lack peaks on CV). Based on the electroanalytical investigations and literature data [38, 51-52], we proposed a mechanism of quercetin oxidation (scheme 1).

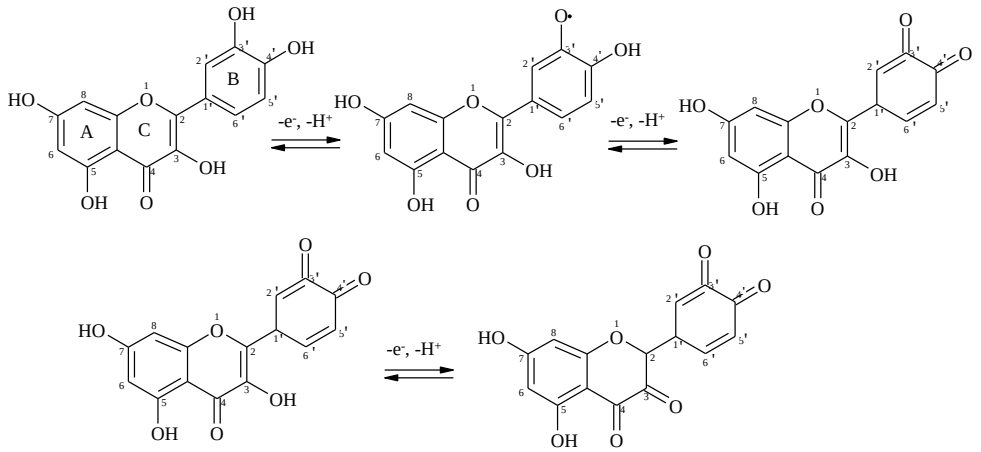

Scheme 1. The electrochemical oxidation reaction of quercetin.

The property and antioxidant capacity studies of quercetin using experiments and theoretical calculation methods can contribute to the ongoing interest in understanding quercetin to better exploit it in the field of biology and food science.

3.5. Cyclic voltammetry of quercetin and *after thermooxidation and UV irradiation.*

The effects of UV radiation, thermo-oxidation stability and antioxidant properties of quercetin were tested. Antioxidant quercetin, quercetin after UV and thermooxidation were examined using CV and DPV methods, which are shown in Figure 8. The voltammetric curves determined the half-wave potential ($E_{1/2}$) of the CV and peak potential (E_p) of DPV. Based on the studies, it can be concluded that the quercetin after UV exposure and thermooxidation had worse antioxidant properties than that before these processes, which is evidenced by the values of $E_{1/2}$ and E_p observed. For quercetin, $E_{1/2}$ CV and E_p with DPV are 0.68 V and 0.64 V, respectively, whereas after UV exposure and thermo-oxidation, $E_{1/2}$ and E_p are more positive (0.75 V and 0.68 V, respectively).

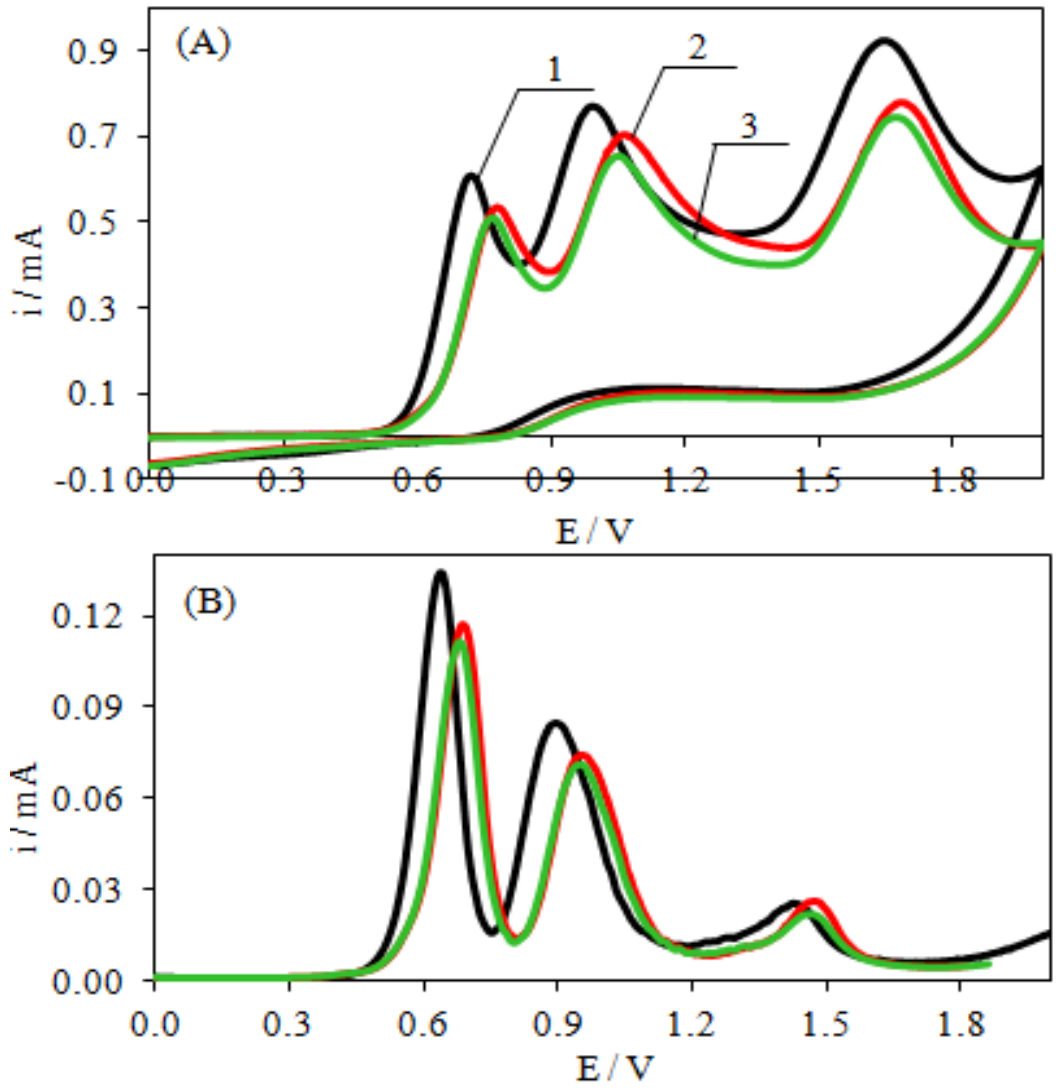

Figure 8. Voltammograms of compounds oxidation at Pt electrode, (A) – CV, (B) – DPV; c = 2 x 10-3 mol L^{-1} in 0.1 mol L^{-1} $(C4H9)_4NClO_4$ in acetonitrile, v = 0.1 V s^{-1}, curve 1 – quercetin, 2 – quercetin after UV irradtaion, 3 – quercetin after thermooxidation.

This result indicates that the antioxidant properties of quercetin deteriorate after UV irradiation and thermooxidation.

3.5. Effects of UV irradiation and thermooxidation on ABTS and DPPH radical scavenging activity of quercetin

ABTS and DPPH are very often used for measure the antioxidant capacities in the food and by agricultural science. The proton radical scavenging reaction is typical method for determination various mechanisms of antioxidant activity. Both DPPH and ABTS are stable free radicals that dissolve in ethanol, and their colors show the characteristic absorption at wavelengths of 519 nm and 734 nm, respectively. The Figure 9 shows the antioxidant activity values of the DPPH and ABTS radical scavenging activity of quercetin. Quercetin can effectively scavenge DPPH and ABTS radicals. Quercetin after UV irradiation and thermooxidation has obviously less scavenging activity than quercetin before the ageing process, which indicates that quercetin after thermal or UV degradation is a much weaker free-radical scavenger and antioxidant than quercetin.

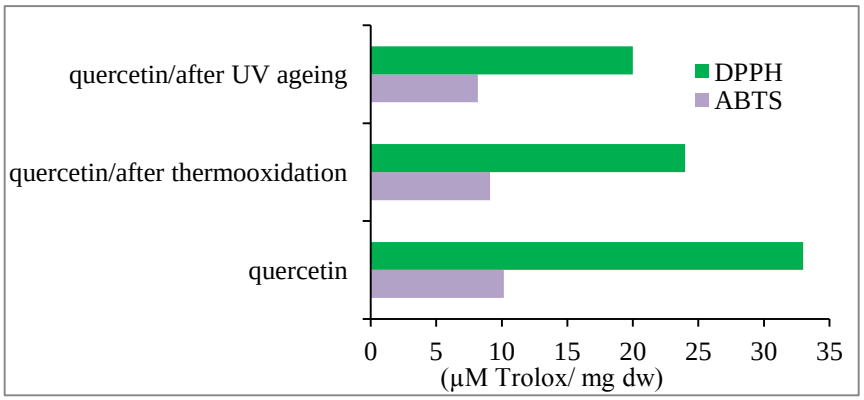

Figure 9. Antioxidant capacity tested by using ABTS and DPPH methods for quercetin.

3.6. FTIR spectroscopy and DSC of quercetin

Figure 10 is a typical FTIR spectrum of an quercetin compund for the band region between 3700 and 700 cm $^{-1}$. Solimani indicated that the carbonylic peak at 1666 cm^{-1} is characetristic for cyclic, conjugate object as benzopyranic-4-one structure. The absorption band at 1522 cm^{-1} is shown benzene ring. Asymmetric stretch of C-O-C group is present in FTIR spectrum at 1198cm^{-1}. The bands at 1351 and 1159 cm^{-1} show C-OH deformation vibration. After UV and thermal ageing we did not notice any significant changes in the structure of quercetin. Only after UV and thermooxidation we observed a small reduction in the band intensity of C-OH group at 1164 cm^{-1} and at the range 3420 cm^{-1}.

On the base thermogram (TGA) we set thermal stability of quercetin (Figure 11).

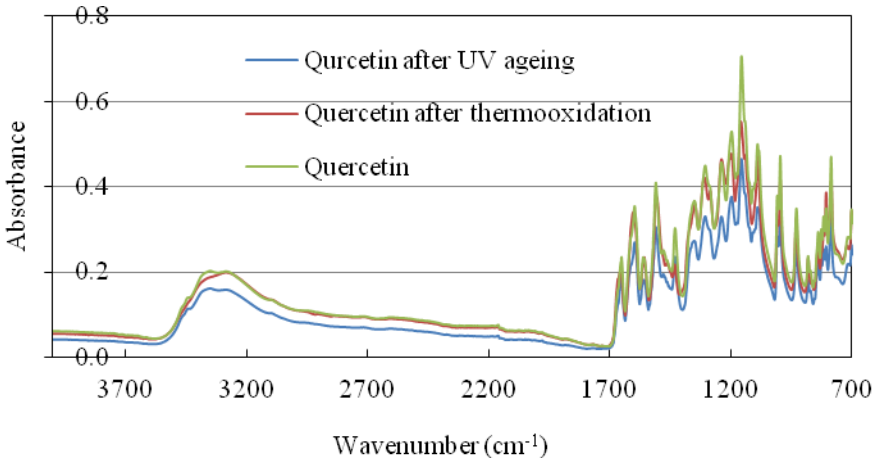

Figure 10. FTIR spectrum of quercetin.

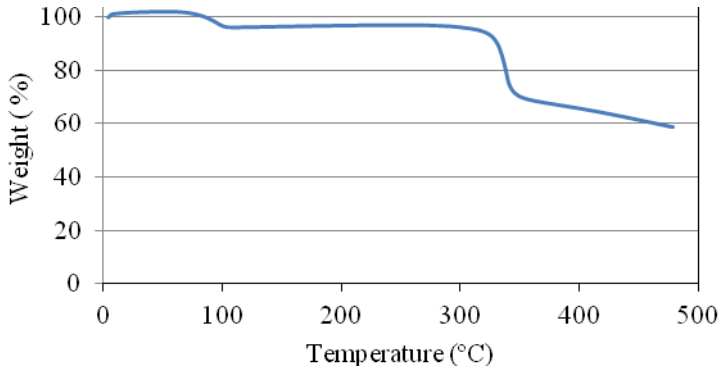

Figure 11. Thermogravimetry analysis of quercetin.

The TG isothermal profile of quercetin showed that this antioxidant present two decopompostion steps. The weight loss between 40 and 160 ºC is due to the absorbed water. The second step is presented after 280 ºC. 38.32% weight loss is attributed to slow degradation of quercetin. Thermogravimetry analysis indicated high thermal stability of this compound.

4. CONCLUSIONS

The electrooxidation behavior of quercetin at the Pt electrode in a non-aqueous solution proceeds in at least three electrode steps before the potential approaches the electrolyte decomposition value. In the first and second steps, the hydroxyl groups of ring B are oxidized. The first step of the electrooxidation process of quercetin includes the exchange of one electron and one proton, which results in the formation of a semiquinone. The next step is the exchange of a second electron and a second proton, which results in the formation of a quinone. In the third electrode step, the hydroxyl group of ring C is oxidized at a more positive potential. Based on the results, the role of the B-ring is to dominate the antioxidant property of quercetin.

The dependence of the anodic peak current vs. the quercetin concentration is linear and can be applied to determine the substrate concentration in environmental samples. The calculated parameters of quercetin electrooxidation are as follows: anodic charge transfer coefficient (βn_β) – 0.51±0.05 and heterogeneous rate constant – (4.5±0.2) × 10^{-4} cm s^{-1} (determined at $E_{1/2}$). Thus, the investigated process proceeds according to the EC mechanism.

The electrooxidation mechanisms of quercetin were proposed. UV treatment and heat storage promoted changes in quercetin antioxidant activity. After irradiation with a wavelength of 340 nm and thermooxidation of antioxidant the activity of quercetin was decreased by approximately ~15%. The effect on the UV-A exposure of the tested flavonoid was notably low. The stability of quercetin against photooxidation and thermooxidation is relatively high. FTIR spectrum of antioxidant after ageing indicated no significant changes in the structure. Quercetin exhibits good antioxidant properties such as being a natural stabiliser for different applications.

ACKNOWLEDGEMENT

This study was supported by Ministry of Science of Higher Education IP 2012 037072

References

1. S. F. Nabavi, G. L. Russo, M. Daglia and S. M. Nabavi, *Food Chem.*, 179 (2015) 305.
2. S. K. Pandeya, D. K. Patelb, R. Thakurc, D. P. Mishrac, P. Maitib and Ch. Haldar, *Int. J. Biol. Macromol.*, 75 (2015) 521.
3. C. Sandoval-Acuña, C. Lopez-Alarcón, M. E. Aliaga and H. Speisky, *Chem. Biol. Interact.*, 199 (2012) 18.
4. R. Kleemann, L. Verschuren, M. Morrison, S. Zadelaar, M. J. van Erk, P. Y. Wielinga and T. Kooistra, *Atherosclerosis*, 218 (2011) 44.
5. A. P. Rogerio, C. L. Dora, E. L. Andrade, J. S. Chaves, L. F .C. Silva, E. Lemos-Senna and J. B. Calixto, *Pharmacol. Res.*, 61 (2010) 288.
6. W. Wiczkowski, D. Szawara-Nowak, J. Topolska, K. Olejarz, H. Zieliński and M. K. Piskuła, *J. Funct. Foods*, 11 (2014) 121.
7. R. Ravichandran, M. Rajendran and D. Devapiriam, *Food Chem.*, 146 (2014) 472.
8. G. Ziyatdinova and H. Budnikov, *Monatsh. Chem.*, (2015) doi:10.1007/s00706-014-1376-5.
9. H. Z. Zare and N. Nasirizadeh, *Electrochim. Acta*, 56 (2011) 3920.
10. A. Masek, E. Chrzescijanska, A. Kosmalska and M. Zaborski, *C. R. Chimie*, 15 (2012) 424.
11. D. Zielinska, B. Pierozynski and W. Wiczkowski, *J. Electroanal. Chem.*, 640 (2010) 23.
12. M. Zidan, R. M. Zawawi, M. Erhayem and A. Salhin, *Int. J. Electrochem. Sci.*, 9 (2014) 7605.
13. A. Masek, E. Chrzescijanska and M. Zaborski, *Int. J. Electrochem. Sci.*, 9 (2014) 7904.
14. H. M. Elqudaby, G. G. Mohamed and G. M. G. El Din, *Int. J. Electrochem. Sci.*, 9 (2014) 856.
15. N. F. Atta, A. Galal and S. M. Azab, *Int. J. Electrochem. Sci.*, 6 (2011) 5082.
16. E. Wudarska, E. Chrzescijanska, E. Kusmierek and J. Rynkowski, *Electrochim. Acta*, 93 (2013) 189.
17. A. Masek, E. Chrzescijanska and M, Zaborski, *Electrochim. Acta*, 107 (2013) 441.
18. E. Chrzescijanska, E. Wudarska, E. Kusmierek and J. Rynkowski, *J. Electroanal. Chem.*, 713 (2014) 17.
19. G. Ziyatdinova, E. Ziganshina and H. Budnikov, *Electrochim. Acta*, 145 (2014) 209.
20. A. Masek, E. Chrzescijanska, M. Zaborski and M. Maciejewska, *C. R. Chimie*, 15 (2012) 524.
21. B. J. Sanghavi, O. S. Wolfbeis, T. Hirsch and N. S. Swami, *Microchim. Acta*, 182 (2015) 1.
22. E. Chrzescijanska and E. Kusmierek, *J. Photochem. Photobiol., A*, 257 (2013) 5.

23. Y. Li and S. M. Chen, *Int. J. Electrochem. Sci.*, 7 (2012) 2175.
24. A. Masek, E. Chrzescijanska and M, Zaborski, *Food Chem.*, 127 (2011) 699.
25. A. Masek, E. Chrzescijanska and M. Zaborski, *Electrochim. Acta*, 107 (2013) 441.
26. G. Ziyatdinova, E. Ziganshina and H. Budnikov, *Talanta*, 125 (2014) 378.
27. D. Mihaylova and S. Schalow, *Braz. Arch. Biol. Technol.*, 56 (2013) 431.
28. T. Siatka and M. Kašparová, *Molecules*, 15 (2010) 9450.
29. B. Tadolini, C. Juliano, L. Pui, F. Franconi and L. Cabrini, *Free Rad. Res.*, 22 (2000) 105.
30. R. Re, N. Pellegrini, A. Proggente, A. Pannala, M. Yang and C. Rice-Evans, *Free Radical Biol. Med.*, 26 (1999) 1231.
31. J. Sochor, J. Dobes, O. Krystofova, B. Ruttkay-Nedecky, P. Babula, M. Pohanka, T. Jurikova, O. Zitka, V. Adam, B. Klejdus and R. Kizek, *Int. J. Electrochem. Sci.*, 8 (2013) 8464
32. A. Masek, E. Chrzescijanska and M. Zaborski, *Food Chem.*, 156 (2014) 353.
33. M. Šeruga, I. Novak and L. Jakobek, *Food Chem.*, 124 (2011) 1208.
34. B. K. Głód, I. Kiersztyn and P. Piszcz, *J. Electroanal. Chem.*, 719 (2014) 24.
35. A. S. Arribas, M. Martínez-Fernández and M. Chicharro, *TrAC, Trends Anal. Chem.*, 34 (2012) 78.
36. A. Masek, E. Chrzescijanska and M. Zaborski, *Int. J. Electrochem. Sci.*, 10 (2015) 2504.
37. H. Yin, Q. Ma, Y. Zhou, S. Ai and L. Zhu, *Electrochim. Acta*, 55 (2010) 7102.
38. A. K. Timbola, C. D. Souza, C. Soldi, M. G. Pizzolatti and A. Spinelli, *J. Appl. Electrochem.*, 37 (2007) 617.
39. B. Dogan-Topal, B. Bozal-Palabıyık, B. Uslu and S. A. Ozkan, *Sens. Actuators, B*, 177 (2013) 841.
40. A.J. Bard, L.R. Faulkner, Electrochemical Methods, Fundamentals and Applications, 2nd ed., John Wiley & Sons, New York, 2001.
41. M. Mazloum-Ardakani and Z. Taleat, *Int. J. Electrochem. Sci.*, 4 (2009) 694.
42. J. A. Harrison and Z. A. Khan, *J. Electroanal. Chem. Interfacial Electrochem.*, 28 (1970) 131.
43. R. S. Nicholson and I. Shain, *Anal. Chem.*, 36 (1964) 706.
44. M. L. Yola, V. K. Gupta, T. Eren, A. E. Şen and N. Atar, *Electrochim. Acta*, 120 (2014) 204.
45. O. A. Farghaly, R. S. Abdel Hameed and Abd-Alhakeem H. Abu-Nawwas, *Int. J. Electrochem. Sci*., 9 (2014) 3287.
46. E. Chrzescijanska, E. Kusmierek and G. Nawrat, *Polish J. Chem.*, 83 (2009) 1115.
47. Z. Galus, Fundamentals of electrochemical analysis, New York: Ellis Horwood; Warsaw: Polish Scientific Publishers PWN, 1994.
48. W. Cai, Y. Chen, L. Xie, H. Zhang and Ch. Hou, *Eur. Food Res. Technol.*, 238 (2014) 121.
49. P. Žižková, D. Blaškovič, M. Májeková, L. Švorc, L. Račková, L. Ratkovská, M. Veverka and L. Haráková, *Mol. Cell. Biochem.*, 386 (2014) 1.
50. A. M. O. Brett and M. E. Ghica, *Electroanalysis*, 15 (2003) 1745.
51. B. Pierozynski and D. Zielinska, *Int. J. Electrochem. Sci.*, 5 (2010) 1507.
52. K. Reddaiah, T. M. Reddy, P. Raghu and B. E. Kumara Swamy, *Anal. Bioanal. Electrochem.*, 4 (2012) 122.